

# Wall Matters: Rethinking the Effect of Wall for Wireless Sensing

BINBIN XIE, University of Massachusetts Amherst, USA MINHAO CUI, University of Massachusetts Amherst, USA DEEPAK GANESAN, University of Massachusetts Amherst, USA JIE XIONG, University of Massachusetts Amherst, USA

Wireless sensing has demonstrated its potential of utilizing radio frequency (RF) signals to sense individuals and objects. Among different wireless signals, LoRa signal is particularly promising for through-wall sensing owing to its strong penetration capability. However, existing works view walls as a "bad" thing as they attenuate signal power and decrease the sensing coverage. In this paper, we show a counter-intuitive observation, i.e., walls can be used to increase the sensing coverage if the RF devices are placed properly with respect to walls. To fully understand the underlying principle behind this observation, we develop a through-wall sensing model to mathematically quantify the effect of walls. We further show that besides increasing the sensing coverage, we can also use the wall to help mitigate interference, which is one well-known issue in wireless sensing. We demonstrate the effect of wall through two representative applications, i.e., macro-level human walking sensing and micro-level human respiration monitoring. Comprehensive experiments show that by properly deploying the transmitter and receiver with respect to the wall, the coverage of human walking detection can be expanded by more than 160%. By leveraging the effect of wall to mitigate interference, we can sense the tiny respiration of target even in the presence of three interferers walking nearby.

CCS Concepts: • **Human-centered computing** → *Ubiquitous and mobile computing systems and tools.* 

Additional Key Words and Phrases: Through-wall sensing, Sensing coverage, Contact-free, LoRa

#### **ACM Reference Format:**

Binbin Xie, Minhao Cui, Deepak Ganesan, and Jie Xiong. 2023. Wall Matters: Rethinking the Effect of Wall for Wireless Sensing. *Proc. ACM Interact. Mob. Wearable Ubiquitous Technol.* 7, 4, Article 190 (December 2023), 22 pages. https://doi.org/10. 1145/3631417

## 1 INTRODUCTION

Recent years have witnessed an explosion of wireless sensing research [10, 25, 33], ranging from coarse-grained activity recognition to fine-grained vital signs monitoring. In the last few years, through-wall sensing [13, 15, 28, 35, 43–45] has attracted particular attention in a variety of applications such as disaster rescue [8] and vehicle-based through-obstruction sensing [27]. In disaster rescue, the capability to sense survivors trapped deep under collapsed structures in a contact-free manner would save precious lives. For smart vehicles, detecting vehicles and pedestrians in the occluded regions can greatly reduce the chance of accidents and injuries.

Among those wireless technologies used for sensing, LoRa has become the mainstream choice for through-wall sensing [8, 39] owing to its large transmission distance (i.e., kilometers) and strong penetration capability [16].

Authors' addresses: Binbin Xie, College of Information and Computer Sciences, University of Massachusetts Amherst, USA, binbinxie@cs. umass.edu; Minhao Cui, College of Information and Computer Sciences, University of Massachusetts Amherst, USA, minhaocui@cs.umass.edu; Deepak Ganesan, College of Information and Computer Sciences, University of Massachusetts Amherst, USA, dganesan@cs.umass.edu; Jie Xiong, College of Information and Computer Sciences, University of Massachusetts Amherst, USA, jxiong@cs.umass.edu.

Permission to make digital or hard copies of all or part of this work for personal or classroom use is granted without fee provided that copies are not made or distributed for profit or commercial advantage and that copies bear this notice and the full citation on the first page. Copyrights for components of this work owned by others than the author(s) must be honored. Abstracting with credit is permitted. To copy otherwise, or republish, to post on servers or to redistribute to lists, requires prior specific permission and/or a fee. Request permissions from permissions@acm.org.

@ 2023 Copyright held by the owner/author(s). Publication rights licensed to ACM. 2474-9567/2023/12-ART190 \$15.00

https://doi.org/10.1145/3631417

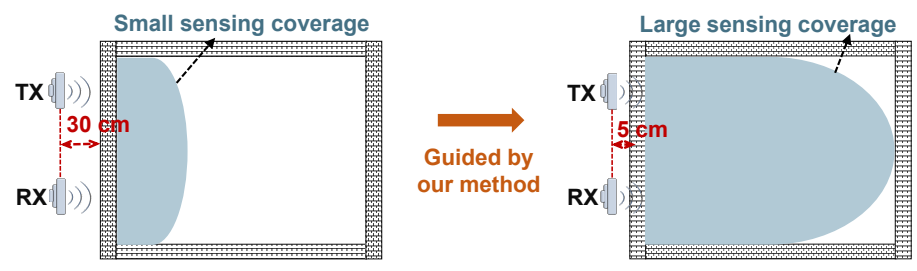


Fig. 1. The sensing coverage can be greatly enlarged via device deployment.

Recent works show that LoRa signals could penetrate multiple walls to sense the subtle chest movement for respiration monitoring [31, 34]. However, in these systems, walls are simply considered as "bad" because they decrease signal power and accordingly reduce sensing coverage [19]. These systems do not study how exactly the walls affect through-wall sensing.

In this paper, we show that the effect of wall on sensing is more complicated than we thought and walls do not always decrease the sensing coverage. Whether a wall decreases or increases the sensing coverage is dependent on how the sensing devices are placed with respect to the wall. Therefore, walls can be smartly leveraged to deal with small sensing coverage and severe interference, which are two critical issues associated with wireless sensing. Specifically, we can use the wall to increase the sensing coverage. We can also use the wall to decrease the sensing coverage if we want to confine sensing within a particular area to mitigate interference. To achieve these objectives, we ask three questions in this work:

- How to model the effect of wall for through-wall sensing?
- What are the key factors affecting the sensing coverage?
- How to control the sensing coverage leveraging the effect of wall to meet practical needs?

First, by taking walls into consideration and developing the through-wall sensing model, we gain a deeper understanding of the effect of wall. When there is no wall in between, the target reflection signal path is composed of two parts, i.e., from transmitter to target, and from target to receiver. On the other hand, in through-wall scenarios, four parts need to be considered, i.e., from transmitter to wall, from wall to target, from target to wall, and finally from the wall to receiver. For each part, we model how the signal propagates and changes. The through-wall sensing model quantifies how the location of wall with respect to the transmitter, receiver and target affects the sensing coverage.

We then characterize the sensing coverage based on the through-wall sensing model. Walls can change both size and shape of the sensing coverage. Specifically, we observe that three key factors affect the sensing coverage in through-wall scenarios. The first factor is *wall-device distance*. We observe that when we move the devices very close to a wall, the sensing coverage becomes much larger. The second factor is *transmitter-receiver distance*. When we increase the distance between the transmitter and receiver, the sensing coverage gets increased first and then decreased. The third one is *the number of walls*. The sensing coverage becomes smaller with more walls in between.

By deeply understanding the effect of walls, we propose novel methods to control the size of sensing coverage. We can achieve a much larger coverage by tuning the three factors via properly placing the transmitter and receiver with respect to the wall. As shown in Fig. 1, by moving the transmitter and receiver closer to the wall, we can significantly enlarge the sensing coverage. It is interesting to see that a very small sensing coverage can also be achieved by varying the transmitter/receiver distance with respect to the wall. We can leverage this small sensing coverage which is conventionally considered as a disadvantage to confine sensing within an area

of interest or to mitigate interference. We thus provide flexibility to adapt the sensing coverage to meet the requirements of different scenarios for through-wall sensing. To summarize, we make the following contributions:

- To the best of our knowledge, this is the first work that challenges the traditional view of "bad" impact of wall on sensing and reveals the fact that wall can be leveraged to benefit sensing. As walls are common in indoor environments, the proposed model helps people understand the effect of wall, pushing wireless sensing one step forward towards real-world adoption.
- We propose to smartly leverage walls to deal with small sensing coverage and severe interference, which are two critical issues associated with wireless sensing.
- We conduct experiments with LoRa platform to demonstrate the effectiveness of the proposed theories. Through properly placing the devices with respect to the wall, the coverage of human walking detection can be expanded by 160% compared to conventional deployment strategies. For interference mitigation, we are able to sense tiny respiration of a target in the presence of three interferers walking nearby, leveraging the effect of wall.

#### 2 PRELIMINARIES

In this section, we introduce the basics of LoRa, through-wall sensing, and the sensing coverage without a wall.

## 2.1 LoRa Primer

LoRa adopts chirp spread spectrum (CSS) modulation technique, which modulates symbols with chirps. The frequency of a LoRa chirp increases (i.e., upchirp) linearly over time at a constant rate. The LoRa receiver demodulates received signals by focusing the power of all the signal samples in the upchirp at one frequency, significantly improving the signal-to-noise ratio (SNR) [16]. Therefore, LoRa can receive weak signals even 20 dB below the noise floor, and also achieves a long communication range (i.e., several kilometers in the rural area). Compared to other wireless signals such as WiFi, LoRa also enables a much larger sensing range and stronger penetration capability [31, 39], making it well-suited for through-wall sensing applications.

#### 2.2 Through-wall Sensing

Now we introduce the rationale of through-wall sensing without attaching any sensors to the target. Considering the scenario in Fig. 2, where there is one target, one wall and one desk in the environment. The LoRa signal goes directly from the transmitter to the receiver, and also gets reflected from the target and nearby objects such as the wall and desk. The target reflection signal penetrates the wall. The signal paths arriving at the receiver can be grouped into two categories, i.e., static path and dynamic path. The dynamic path is the target reflection path while the static paths are composed of the line-of-sight (LoS) path and reflected paths from the wall and desk. The rationale behind through-wall sensing is that the target reflection signals vary with target movement, and by analyzing the signal variation at the receiver, the target movement can be inferred.

# Sensing Coverage Model without A Wall

Consider a simple scenario as shown in Fig. 3(a) where the target reflection signal path highlighted in red is divided into two parts (i.e.,  $TX \rightarrow Target$  and  $Target \rightarrow RX$ ). We denote the distance between the transmitter and target as  $d_1$ , and the distance between target and receiver as  $d_2$ . By applying the Friis equation [1, 11, 14] to the first part (TX  $\rightarrow$  Target), we can obtain the signal power arriving at the target as

$$P_{tx \to tar} = P_T \cdot G_T \cdot \frac{1}{4\pi (d_1)^2},\tag{1}$$

<sup>&</sup>lt;sup>1</sup>We use *dynamic signal* and *target reflection signal* interchangeably in this paper.

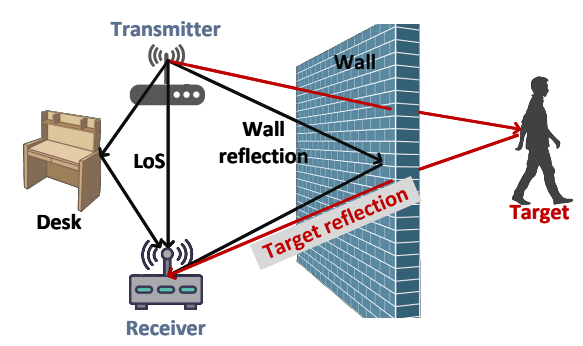


Fig. 2. A sample through-wall sensing scenario.

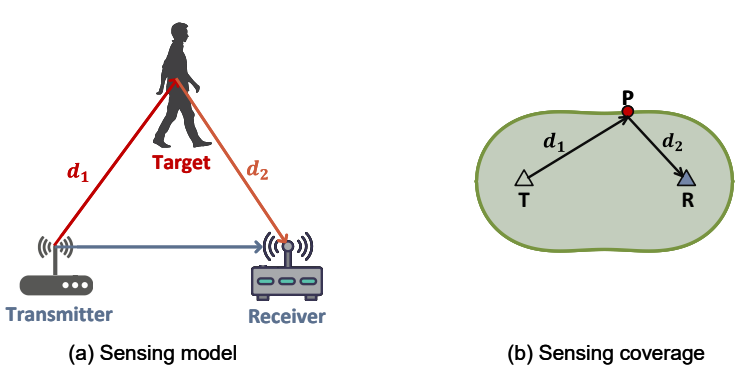


Fig. 3. Sensing model without wall.

where  $P_T$  is the transmission power and  $G_T$  is the antenna gain of the transmitter. When the signal reflected by the target reaches the receiver, i.e., the second part (Target  $\rightarrow$  RX), we can get the power  $P_{tar}$  of target reflection signal at the receiver

$$P_{tar} = P_{tx \to tar} \cdot \sigma \cdot \frac{1}{4\pi (d_2)^2} \cdot A_R = \frac{P_T G_T A_R \sigma}{(4\pi)^2 (d_1 d_2)^2},$$
 (2)

where  $\sigma$  is the radar cross section (RCS) of the target. It contains the ratio between the power reflected by the target and the power incident on the target [6, 20].  $A_R = \frac{G_R \lambda^2}{4\pi}$ , where  $G_R$  is the antenna gain of receiver and  $\lambda$  is the signal wavelength. In Eq. (2), all the parameters can be considered as constants, except for  $d_1$  and  $d_2$ . Therefore, the power of target reflection signal is mainly determined by the product of two distances, i.e.,  $d_1d_2$ .

Since the sensing coverage is closely related to the power of target reflection signal, we can use  $d_1d_2$  to model the size of sensing coverage without a wall [25]. Specifically, on the boundary of sensing coverage, the power of target reflection signal is the minimum for sensing. The product of distances  $d_1d_2$  on the sensing boundary is a constant. Fig. 3(b) shows one example for sensing coverage highlighted in green where T and R represent the locations of transmitter and receiver. P is the target location on the sensing coverage boundary.

#### 3 UNDERSTANDING THE EFFECT OF WALL ON THROUGH-WALL SENSING

In this section, we investigate the effect of wall on the sensing model and sensing coverage.

## 3.1 Through-wall Sensing Model

Fig. 4 shows two typical through-wall scenarios, i.e., (1) the transmitter and receiver are deployed at the same side of wall (Fig. 4(a)), and (2) the transmitter and receiver are deployed at different sides of wall (Fig. 4(b)). In

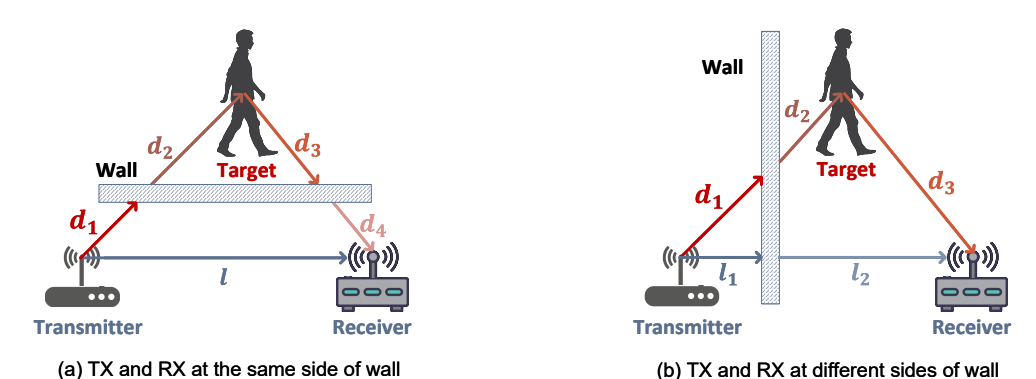


Fig. 4. Through-wall sensing model.

this paper, we use the scenario in Fig. 4(b) to illustrate the impact of wall. The theories developed can also be applied to the scenario in Fig. 4(a). We present how to apply the theories in both scenarios in Section 4.2 and evaluate the effectiveness in Section 5.2.

**Modeling target reflection signal.** Different from the sensing model without a wall which only involves two distances, i.e., transmitter-target distance and target-receiver distance, we need to consider more distances depending on the location of wall in through-wall sensing model. Take the scenario in Fig. 4(b) as an example. The wall divides the signal path between the transmitter and target into two segments, i.e., transmitter-wall distance  $d_1$  and wall-target distance  $d_2$ . The target-receiver distance is denoted as  $d_3$ . Now three distance segments instead of two are considered in the through-wall sensing model.

Based on the Friis transmission equation [1], the signal power arriving at the wall (i.e.,  $TX \rightarrow Wall$ ) in Fig. 4(b) can be modeled as

$$P_{tx \to wall} = P_T \cdot G_T \cdot \frac{1}{4\pi (d_1)^2},\tag{3}$$

where  $P_T$  is the transmission power and  $G_T$  is the antenna gain of the transmitter. Then we model the signal power for the second part (i.e., Wall  $\rightarrow$  Target) as

$$P_{wall \to tar} = P_{tx \to wall} \cdot T_{wall}^2 \cdot \frac{1}{4\pi (d_2)^2} = \frac{P_T G_T T_{wall}^2}{(4\pi)^2 (d_1 d_2)^2},\tag{4}$$

where  $T_{wall}$  represents the transmission coefficient of the occluding wall, which is closely related to the wall thickness and its material. Note that  $T_{wall}$  characterizes the loss caused by wall penetration [19]. Next, for the third part (i.e., Target  $\rightarrow$  RX), the power of target reflection signal at the receiver can be expressed as

$$P_{tar} = P_{wall \to tar} \cdot \sigma \cdot \frac{1}{4\pi (d_3)^2} \cdot A_R = \frac{P_T G_T T_{wall}^2 A_R \sigma}{(4\pi)^3 (d_1 d_2 d_3)^2},$$
 (5)

where  $\sigma$  is the RCS of target, which indicates the ratio between the power reflected by the target and the power incident on the target [6, 20].  $A_R = \frac{G_R \lambda^2}{4\pi}$ , where  $G_R$  is the antenna gain of receiver and  $\lambda$  is the signal wavelength. Now we can see that the power of target reflection signal is determined by the product of three distances  $d_1 d_2 d_3$ . With n walls, the signal path can be divided into n+2 segments, and the power of target reflection signal is determined by the product of n+2 segments. The proposed model takes into account the free-space loss of the target reflection signal as well as the additional loss due to the wall.

**Modeling static signal.** Similarly, by applying the Friis transmission equation, we can obtain the power of static signal  $P_{static}$  based on

$$P_{static} = \frac{P_T G_T T_{wall}^2 A_R}{(4\pi)^2 (l_1 l_2)^2},\tag{6}$$

where  $l_1$  and  $l_2$  are the transmitter-wall distance and wall-receiver distance in Fig. 4(b), respectively.

# 3.2 Through-wall Sensing Coverage Model

To model the through-wall sensing coverage, we need to consider (1) the power of target reflection signal, and (2) the noise power, as both of them determine the sensing coverage. Therefore, we employ a metric, SSNR (sensing-signal-to-noise ratio) [25], to quantify the sensing capability

$$SSNR = \frac{P_{tar}}{P_i},\tag{7}$$

where  $P_{tar}$  denotes the power of target reflection signal, and  $P_i$  is the noise power including both the thermal noise and interference induced by static signal. Note that SSNR is different from SNR. SNR defines the ratio between the power of received signal (including both static signal and target reflection signal) and noise power. In contrast, SSNR cares about the ratio between the power of target reflection signal and noise power.

3.2.1 Characterizing Noise. Besides thermal noise which is the common noise source for wireless communication [9], the static signal is also a noise source in wireless sensing, which affects the sensing coverage. Specifically, the static signal induces additional interference and the effect of such interference is similar to the noise. To explore the impact of static signal, we conduct experiments in an open environment, and vary the distance between transmitter and receiver to change the static signal power. We first apply a Savitzky-Golay filter to denoise the received signal. We calculate the static signal power as the average of the collected signal power within a window of 0.1 s, while the interference power is calculated as the power difference between before and after filtering the received signal. As shown in Fig. 5, we observe that the interference power is in proportion to the static signal power, and the slope is constant after fitting with the least square method. Note that thermal noise is much smaller than the interference caused by the static signal.

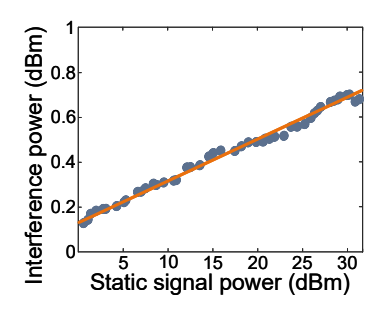


Fig. 5. Interference power caused by static signal.

Therefore, based on Eq. (6), we represent the interference power as

$$P_i = \alpha P_{static} + b = \alpha \frac{K}{(l_1 l_2)^2} + b, \tag{8}$$

where  $\alpha$  is the slope of fitting curve, b is a constant, and  $K = \frac{P_T G_T T_{wall}^2 A_R}{(4\pi)^2}$  is also a constant.

190:7

3.2.2 Sensing Coverage Model. With the target reflection signal power  $P_{tar}$  modeled in Section 3.1 and the interference power  $P_i$  modeled in Section 3.2.1, the SSNR can be rewritten as

$$SSNR = \frac{P_{tar}}{P_i} = \frac{\frac{K\sigma}{4\pi (d_1 d_2 d_3)^2}}{\alpha \frac{K}{(l_1 l_2)^2} + b} = \frac{K\sigma}{4\pi (d_1 d_2 d_3)^2 (\alpha \frac{K}{(l_1 l_2)^2} + b)}.$$
 (9)

In this equation, K is a constant.  $\alpha$  and b can be measured in advance. If the RCS of target  $\sigma$  is assumed to be a constant and b is small, Eq. (9) can be simplified as

$$SSNR \propto \frac{(l_1 l_2)^2}{(d_1 d_2 d_3)^2}. (10)$$

From this equation, we can see that the sensing capability is closely related to the distance segments of the target reflection signal ( $d_1$ ,  $d_2$ , and  $d_3$ ) and distance segments of the static signal ( $l_1$  and  $l_2$ ). Now we investigate how the sensing capability varies with the target location. As shown in Fig. 6, we plot the heatmap of sensing capability for a specific scenario based on our proposed model (Eq. (10)). Red color indicates higher sensing capability while blue color represents lower sensing capability. We can observe that the regions near the devices and the wall have a higher sensing capability.

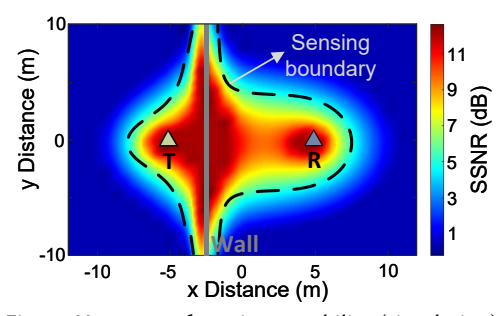


Fig. 6. Heatmap of sensing capability (simulation).

 $SSNR_{min}$  is the minimum SSNR required for sensing at the boundary. Therefore, the sensing boundary can be represented as

$$(d_1 d_2 d_3)_b \propto \sqrt{\frac{(l_1 l_2)^2}{SSNR_{min}}}.$$
 (11)

For a specific sensing application, usually there is a minimum requirement for SSNR. For example, respiration sensing requires an SSNR of 6 dB and human walking detection requires an SSNR of 2 dB. From the equation above, we can see that  $l_1l_2$  affects the sensing boundary. The value of  $l_1l_2$  depends on the wall-device distance and transmitter-receiver distance.

3.2.3 Impact of Multipath. Recall that the received signal is composed of static signals reflected from nearby static objects and dynamic signal reflected from the target. When environment changes, the static signal gets changed, causing the power of static signal to vary. In this case, the power of interference induced by static signal also changes. Therefore, multipath can cause the interference power to vary, and change the sensing coverage accordingly. We conduct benchmark experiments in Section 5.1 to verify the effect of multipath on sensing coverage.

#### 4 CONTROLLING SENSING COVERAGE FOR THROUGH-WALL SENSING

In this section, we study the key factors affecting the through-wall sensing coverage and explain how to control the sensing coverage to deal with the two well-known issues in wireless sensing, i.e., limited sensing coverage and interference.

# 4.1 Factors Affecting Sensing Coverage

Based on the sensing coverage model described in Section 3.2.2, three factors (i.e., wall-device distance, transmitter-receiver distance, and the number of walls) affect the shape as well as the size of sensing coverage.

#### 4.1.1 Factor I: Wall-Device Distance.

**Observation 1:** The sensing coverage becomes larger when the devices are closer to the walls.

We first investigate the impact of wall-device distance. To do this, we keep the distance between transmitter and receiver as 10 m, and decrease the wall-transmitter distance from 9.5 m to 0.5 m. To make sure only the wall-transmitter distance is changed, we keep the transmitter-receiver distance fixed, and move the transmitter and receiver at the same time. We plot the sensing coverage<sup>2</sup> based on our proposed model (Eq. (11)) as shown in Fig. 7. We can see that the size and shape of sensing coverage get changed when the location of wall varies with respect to the transmitter and receiver. More interestingly, the sensing coverage is larger when the wall is closer to either the receiver (Fig. 7(a)) or transmitter (Fig. 7(g)). Note that in Fig. 7(a), the wall-transmitter distance is 9.5 m and the wall is only 0.5 m to the receiver. Therefore, we can conclude that the sensing coverage becomes larger when the devices (i.e., transmitter or/and receiver) are closer to the wall.

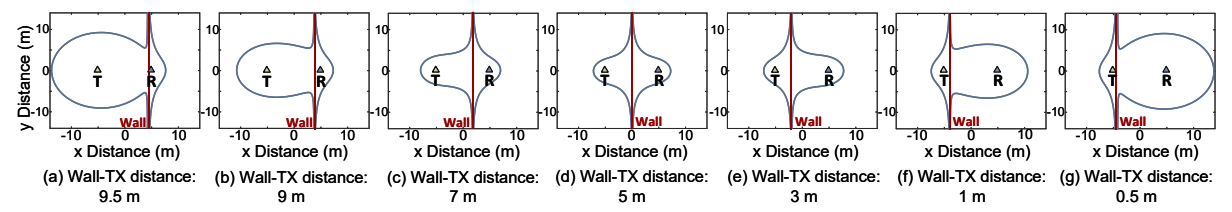


Fig. 7. Impact of wall-device distance on sensing coverage.

The reason behind this phenomenon is explained with one simple example. Fig. 8 shows two cases with different wall-transmitter distances. The wall is closer to the transmitter in Case II. As we can see, the target-receiver distances in the two cases are the same, i.e.,  $d_{3a}=d_{3b}$ , while the transmitter-wall distance  $d_{1a}>d_{1b}$  and the wall-target distance  $d_{2a}< d_{2b}$ . When  $d_{1a}+d_{2a}=d_{1b}+d_{2b}$ , we can obtain  $d_{1a}\cdot d_{2a}>d_{1b}\cdot d_{2b}$ . Therefore, the relationship of the products of three distances in two scenarios is  $d_{1a}\cdot d_{2a}\cdot d_{3a}>d_{1b}\cdot d_{2b}\cdot d_{3b}$ . According to Eq. (5), with a smaller product of three distances in Case II, the power of target reflection signal is larger. Therefore, the sensing coverage is larger in Case II when the wall is closer to transmitter.

Based on this observation, we know that the sensing coverage is the largest when we attach the devices to the walls (i.e., the minimum wall-device distance). We study the effect when the devices are attached to the walls in the evaluation section (Section 5.2).

#### 4.1.2 Factor II: Transmitter-Receiver Distance.

**Observation 2:** With the transmitter-receiver distance increasing, the sensing coverage increases first, and then decreases. When the transmitter-receiver distance is increased further, the sensing coverage collapses into several separate areas distributed around the transmitter, receiver and wall.

 $<sup>^{2}</sup>$ Note that the sensing coverage shown in Section 4 is only for respiration sensing, and we study the sensing coverage for walking sensing in the evaluation section (Section 5).

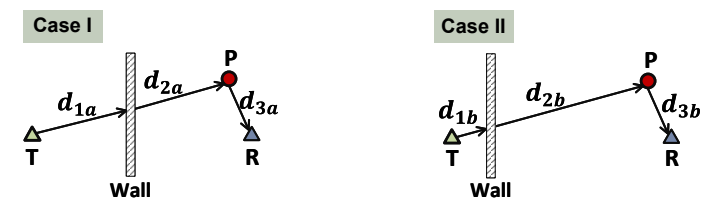


Fig. 8. Two cases with the same transmitter-target-receiver distances but different wall-device distances.

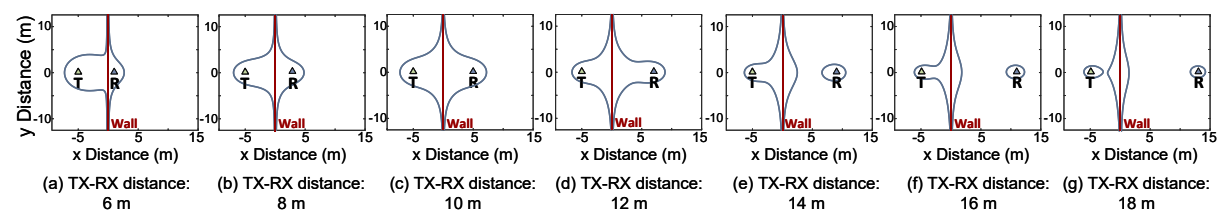


Fig. 9. Impact of transmitter-receiver distance on sensing coverage.

To investigate the impact of the transmitter-receiver distance, we keep the locations of wall and transmitter fixed, and move the receiver to increase the transmitter-receiver distance from 6 m to 18 m with a step size of 2 m. The wall-transmitter distance is 5 m. Fig. 9 presents the corresponding sensing coverages under different transmitter-receiver distances. We can see that the size of sensing coverage increases first, and then decreases. Specifically, when the distance between transmitter and receiver is small, e.g., 6 m, the sensing coverage is limited. This is because the static signal is much stronger, and results in a larger interference power. More interestingly, when the transmitter-receiver distance is very large, e.g., 18 m as shown in Fig. 9(g), the sensing coverage is smaller, and only distributed around the wall, transmitter and receiver. In this case, we can only sense the human movements near the wall, transmitter and receiver. This property can be leveraged to sense only the region of interest and mitigate interference, which will be detailed in Section 4.2.2. Moreover, we observe that the sensing coverage is not evenly distributed between the transmitter and receiver. This is mainly because the wall-transmitter distance is not exactly the same as the wall-receiver distance.

# 4.1.3 Factor III: Number of Walls.

**Observation 3:** With more walls between the transmitter and receiver, the target reflection signal becomes weaker, resulting in a smaller sensing coverage.

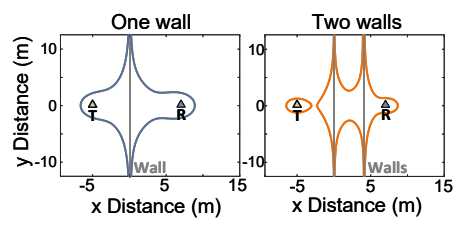


Fig. 10. Impact of number of walls on sensing coverage.

The impact of number of walls on sensing coverage is obvious. The signal attenuation becomes larger as the number of walls increases. We extend the proposed through-one-wall sensing coverage model to that through multiple walls, and plot the corresponding sensing coverage. As shown in Fig. 10, the sensing coverage through two walls is much smaller than that with one wall. Moreover, based on our model, the distance between the

adjacent walls can affect the sensing coverage. However, the wall-wall distance can not be tuned in practice. We can only control the number of walls by placing the transmitter and receiver at different locations.

- 4.1.4 Properties of Through-wall Sensing Coverage. Based on the above analysis, we summarize the key properties of through-wall sensing coverage.
  - The sensing coverage is dependent on the locations of devices with respect to walls.
  - The sensing coverage is the largest when attaching the devices to the wall. By increasing either the wall-transmitter distance or wall-receiver distance, the sensing coverage becomes smaller.
  - When the transmitter-receiver distance is small, the sensing coverage is a single small area. When the transmitter-receiver distance is very large, the sensing coverage becomes several separated small areas surrounding the wall, transmitter and receiver.
  - Increasing the number of walls decreases the size of sensing coverage.

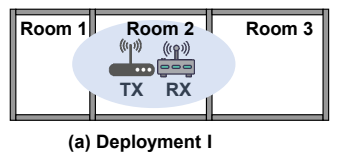
Tuning these factors can vary the size of sensing coverage. In real-life scenarios, it is highly impossible to tune all these factors to be optimal at the same time. We therefore need to make a trade-off between them.

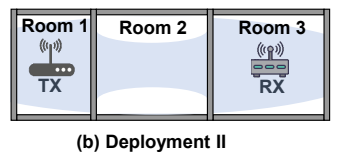
# 4.2 Controlling Sensing Coverage

In this section, we show how to deploy devices to deal with the two critical issues in through-wall sensing, i.e., limited sensing coverage and severe interference.

4.2.1 Enlarging Through-wall Sensing Coverage. To enlarge the sensing coverage, we leverage the properties summarized in Section 4.1.4 to plan device deployment. We consider two cases in the real-life scenarios as described below.

Case I: devices are located inside rooms. As shown in Fig. 11(a), the transmitter and receiver are deployed inside the rooms to sense the target movement. For instance, we place one pair of transmitter and receiver inside an apartment and want to cover the whole apartment for sensing. Fig. 11 shows three device deployments. First, we deploy the transmitter and receiver at the center of whole area as shown in Fig. 11(a). However, only a limited area can be covered due to the small transmitter-receiver distance. To cover a large area, we deploy the transmitter and receiver in different rooms separated by a larger distance as presented in Fig. 11(b). However, the sensing coverage still can not cover the whole area. Further, as shown in Fig. 11(c), we minimize the wall-device distance by attaching transmitter and receiver to the wall. A much larger sensing coverage can now be achieved to cover the whole apartment.





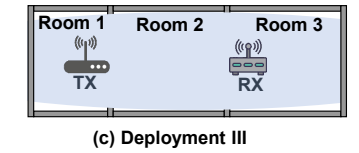


Fig. 11. Enlarging sensing coverage for Case I.

Case II: devices are located outside the rooms. As shown in Fig. 12, we deploy one pair of transmitter and receiver outside the rooms to sense the target movement inside. For instance, the eavesdropper places devices outside a house to track the occupants' daily activities [23]. In this case, directional antennas can be employed to focus sensing at one direction. As shown in Fig. 12(a), when the transmitter and receiver are placed far from the wall, the sensing coverage is small. In Fig. 12(b), by moving the transmitter and receiver closer to the wall, the sensing coverage becomes larger. If we attach the transmitter and receiver to the wall as shown in Fig. 12(c), the sensing coverage can be further increased to cover all the three rooms. Different from the omni-directional antennas which have large static signal power when the transmitter is close to receiver, directional antennas do

not have direct signal from the transmitter to receiver, and thus the static signal power is much smaller. Therefore, in this case, the transmitter-receiver distance has little impact on the size of the sensing coverage.

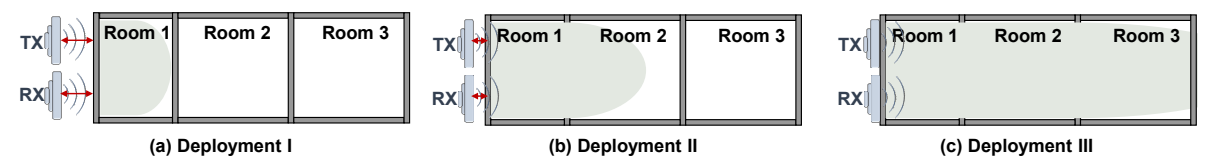


Fig. 12. Enlarging sensing coverage for Case II.

4.2.2 Mitigating Interference. While a larger sensing coverage is usually preferable, it also brings one critical issue, i.e., larger interference area. The interferers can also reflect signals, and these signals as well as the target reflection signal get mixed at the receiver. If this issue is not properly addressed, it can greatly degrade the performance of through-wall sensing in real-world settings. The state-of-the-art approaches generally utilize a large antenna array or a large bandwidth, which can separate the target reflection signal from the interference signal in the spatial domain or time domain. Unfortunately, larger bandwidth and large antenna array are not available on LoRa. The channel bandwidth for LoRa is just 500 kHz and there are usually only two antennas equipped at a LoRa gateway [39].

To address the interference issue, we tune the three factors by planning device placement to constrain sensing only within the area of interest. We utilize one simple scenario in Fig. 13 to demonstrate how to mitigate the impact of interference. As shown in Fig. 13(a), when the transmitter and receiver are close, even though the target is closer to the sensing devices, the interferer can still affect target sensing because the interference region is large [31]. On the other hand, as shown in Fig. 13(b), if we tune the affecting factors, i.e., increasing the transmitter-receiver distance and the wall-device distance, the sensing coverage becomes several smaller regions. The sensing area now only covers the target, and the impact of interference is mitigated. Note that we assume we know the area of interest before we control the sensing coverage. For instance, if we would like to monitor a target in a particular room, we adjust the sensing coverage to just cover this room.

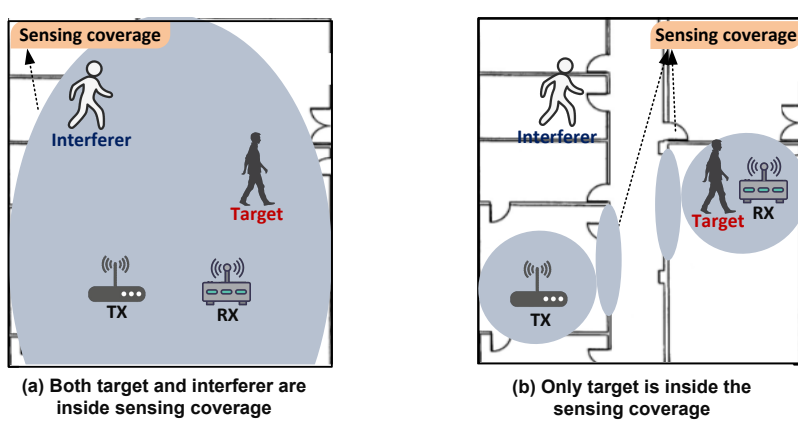


Fig. 13. Interference mitigation with device deployment.

#### 5 EVALUATION

In this section, we first conduct benchmark experiments to verify the key properties of through-wall sensing coverage. Then we evaluate the effectiveness of enlarging sensing coverage and mitigating interference with device placement guided by the model for two applications, i.e., human respiration sensing and walking detection. This project is IRB approved by our institute.

**Hardware setup.** In the experiments, we utilize one LoRa node as the transmitter, and one USRP X310 as the receiver as shown in Fig. 14. The LoRa node is Semtech SX1276 with an Arduino Uno, which is configured to transmit LoRa signal at 915 MHz frequency band with a 125 kHz channel bandwidth. Both the LoRa transmitter and receiver are equipped with one antenna. The default antenna is Proxicast omni-directional antenna with a gain of 5 dBi [2]. The sampling rate of the USRP is set as 500 kHz. A Dell OptiPlex 7050 tower desktop computer with an Intel Core i7 CPU and 16 GB RAM is connected to the receiver via a USB cable to collect signal samples and process the data.

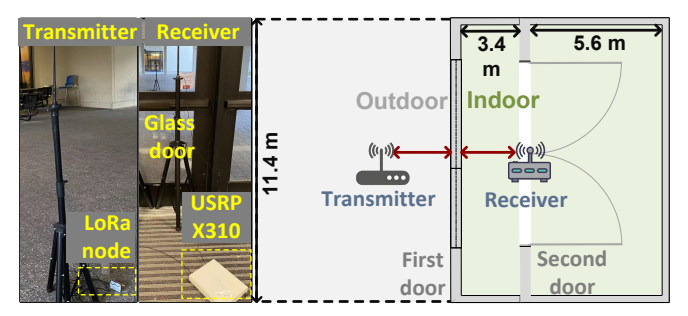


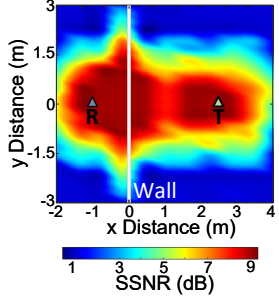
Fig. 14. Benchmark experiment scenario.

## 5.1 Verify Sensing Coverage in Through-wall Scenarios

We first evaluate the spatial distribution of sensing capability in through-wall scenarios. Then, we verify the effect of three key factors on through-wall sensing coverage, i.e., (1) the wall-device distance, (2) the transmitter-receiver distance, and (3) the number of walls.

**Experiment setup.** We conduct experiments at the entrance area of one building as shown in Fig. 14. The receiver is deployed inside the building (i.e., indoors) while the transmitter is located outside the building (i.e., outdoors). Omni-directional antennas are used in the experiments. Two large doors made of glass are employed to act as walls. The distance between two doors is 3.4 m. For the experiments with only one wall, we open the second door to make sure the signal only penetrates the first door. In these experiments, we take respiration sensing as the example to evaluate the sensing coverage, and we choose the target locations where SSNR = 6 dB as the sensing boundary.

Verify spatial distribution of sensing capability. We first conduct experiments to verify the sensing capability at different target locations. There is one wall between the transmitter and receiver. The transmitter-receiver distance is 10 m, and the receiver is placed 2.5 m away from the wall. We employ SSNR to quantify the sensing capability. We divide the 25 m  $\times$  20 m space into 500 grids, and measure the SSNR value in each grid to generate the heatmap of sensing capability as shown in Fig. 15. The red color means a good sensing capability while the blue color indicates a poor sensing capability. The sensing capability near the transmitter, receiver and wall is better than that further away. We can see that the shape and size of sensing area obtained in real-world experiment match the theoretical results in Section 3.2 well.



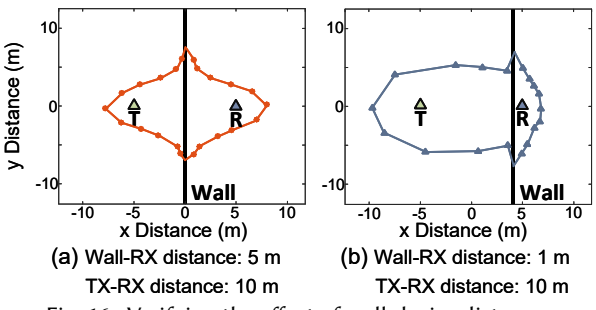


Fig. 15. Spatial distribution of SSNR.

Fig. 16. Verifying the effect of wall-device distance.

Verify effect of wall-device distance. In this experiment, we verify the effect of wall-device distance on the sensing coverage. The transmitter-receiver distance is set as 10 m. To only change the wall-device distance, we keep the transmitter-receiver distance fixed and move the transmitter and receiver at the same time. Fig. 16(a) and (b) show the sensing coverage under two different wall-device distances. As we can see, the sensing coverage becomes larger when the distance between wall and receiver is decreased from 5 m to 1 m. Moreover, the sensing coverages obtained in real-world experiment in Fig. 16(a) and Fig. 16(b) match the theoretical coverages obtained in Fig. 7(d) and Fig. 7(b). These experiment results demonstrate the correctness of the proposed model in Section 4.1.1.

Verify effect of transmitter-receiver distance. We also conduct experiments in the same environment to evaluate the effect of transmitter-receiver distance. As shown in Fig.  $17(a)\sim(d)$ , we keep the transmitter and wall static, and move the receiver to change the transmitter-receiver distance from 6 m to 12 m at a step size of 2 m. We can observe that by increasing the transmitter-receiver distance, the sensing coverage increases first, and then decreases. These results match the theoretical analysis in Section 4.1.2.

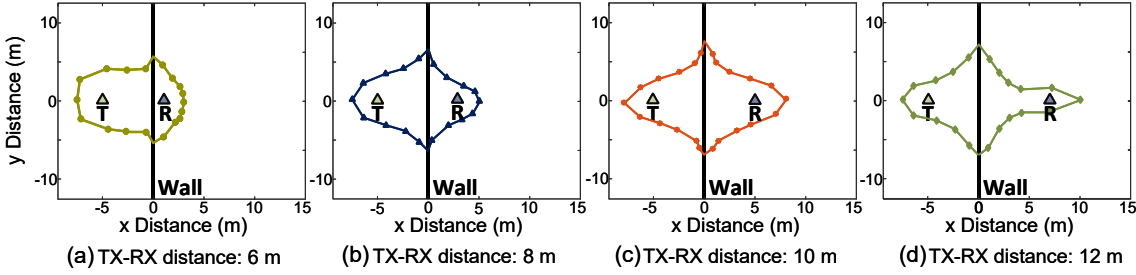


Fig. 17. Verifying the effect of transmitter-receiver distance.

Verify effect of number of walls. Now we conduct experiments to compare the sensing coverage between one wall and two walls. In these two scenarios, we fix the transmitter-receiver distance as 12 m. As shown in Fig. 18(a) and (b), the sensing coverage becomes smaller when there are two walls. The shape of sensing coverage obtained in the experiment also matches the analysis in Section 4.1.3.

Verify effect of multipath. To evaluate the impact of multipath on sensing coverage, we conduct experiments with the setup shown in Fig. 19(a). The transmitter is deployed 1.5 m away from the wall outside the classroom, and the receiver is located in the classroom with a wall-receiver distance of 3.5 m. The wall is made of brick with a thickness of 17.2 cm. To make it easier to evaluate the impact of multipath, we decrease sensing coverage by reducing the transmission power of LoRa node from 20 dBm to 1 dBm. The antenna gain of transmitter and receiver is 5 dBi. We randomly change the chair layout in the classroom to vary the multipath conditions. For each multipath condition, we measure the sensing coverage for respiration sensing.

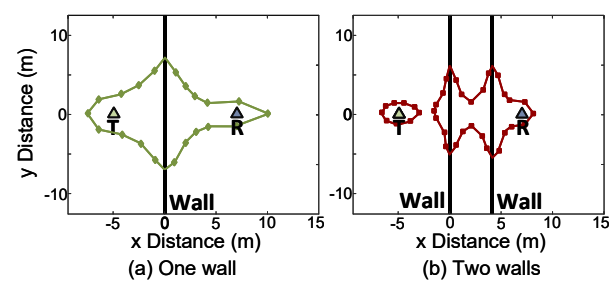


Fig. 18. Verifying the effect of the number of walls.

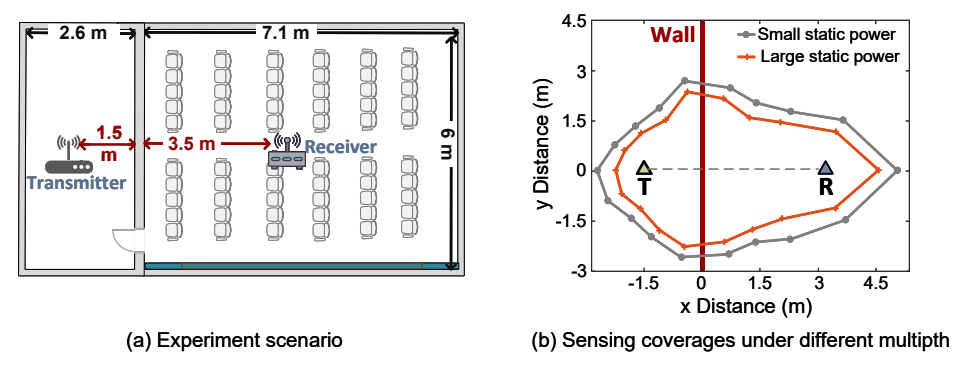


Fig. 19. Verifying the effect of multipath.

As shown in Fig. 19(b), we can observe that when the transmitter and receiver are kept at the same locations, the size of sensing coverage varies under different multipath conditions. The power of static signal power also varies with the multipath. Under the multipath condition with a smaller static signal power, the sensing coverage is larger. This is because the interference power caused by the static signal is smaller. On the other hand, when the static signal power becomes larger, the sensing coverage decreases. The results validate our analysis on the impact of multipath in Section 3.2.3.

# 5.2 Enlarging Through-wall Sensing Coverage

In this section, we conduct experiments with two applications, i.e., respiration sensing and walking detection, to evaluate the effectiveness of leveraging the properties of through-wall sensing identified in this paper to enlarge the sensing coverage.

- 5.2.1 Micro-level Respiration Sensing. We conduct experiments in the scenario with three rooms as shown in Fig. 20. To measure the sensing coverage, we ask the target to stand in each of the three rooms to measure the sensing boundary. The sensing boundary is determined where SSNR = 6 dB. In the experiments, we employ the omni-directional antennas at the receiver and transmitter, and place them at a height of 1.2 m from the ground. By applying the properties summarized in this work to guide the device placement, we can increase the sensing coverage to cover the three rooms. We compare the sensing coverages under five different deployment strategies.
  - S1) As shown in Fig. 21(a), we deploy the transmitter and receiver in the same room (Room 2) with a distance of 2 m. The sensing coverage is highlighted in yellow, and only covers part of Room 2. Target in Room 1 and Room 3 can not be sensed.

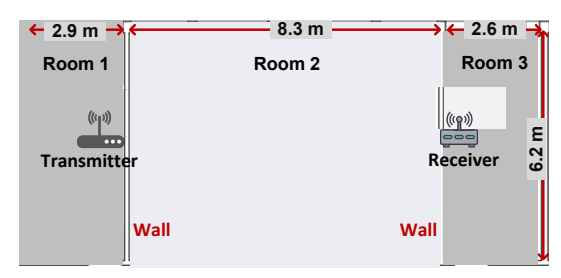


Fig. 20. Experiment scenario with three rooms.

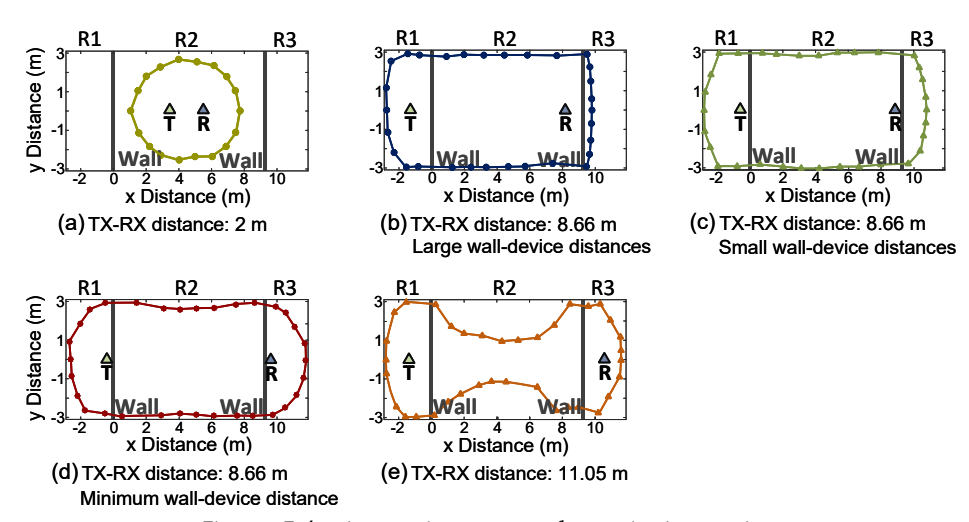


Fig. 21. Enlarging sensing coverage for respiration sensing.

- S2) As shown in Fig. 21(b), we deploy the transmitter and receiver in different rooms, i.e., Room 1 and Room 2, with a distance of 8.66 m. By increasing the transmitter-receiver distance, the sensing coverage becomes much larger which is highlighted in blue. Now we can cover Room 1 and Room 2 for respiration sensing.
- S3) In Fig. 21(c), to further increase the sensing coverage, we decrease the wall-device distances, i.e., attaching the receiver to the wall and reducing transmitter-wall distance to 0.18 m. The transmitter-receiver distance does not change. We observe that the sensing coverage becomes larger.
- S4) As presented in Fig. 21(d), we deploy the transmitter in Room 1 and receiver in Room 3. The two devices are attached to the wall, i.e., minimum wall-device distance. Now we can cover all the three rooms for respiration sensing.
- S5) As shown in Fig. 21(e), if we further increase the transmitter-receiver distance to 11.05 m, the sensing coverage becomes smaller. Moreover, the shape of sensing coverage is also changed. Only part of area in Room 2 is covered.

These experiments show the effectiveness of tuning these key factors to control the sensing coverage for respiration sensing.

5.2.2 Macro-level Walking Detection. We conduct experiments in two scenarios: devices are located inside rooms, and devices are located outside rooms. To measure the sensing coverage for walking detection, we ask the target to walk in each room and check whether we can detect the walking. Since walking induces larger movement compared to respiration, we can detect walking with a smaller SSNR, i.e., 2 dB.

Case I: devices are located inside targeted rooms. Both the transmitter and receiver are equipped with one omni-directional antenna to cover a large direction range. The antennas are Proxicast omni-directional antennas with a gain of 5 dBi. As shown in Fig. 22, we conduct experiments in a large area with a size of  $34.4 \text{ m} \times 6.2 \text{ m}$ . There are 9 rooms inside this area, and the door of each room is closed. As presented in Fig. 22(a), when the transmitter and receiver are deployed in the middle of the area with a distance of 4.2 m, the sensing coverage is relatively small. As shown in Fig. 22(b) and (c), when we deploy the transmitter and receiver in different rooms with a distance of 11.05 m and 14.16 m, the sensing coverages become much larger. To further increase the sensing coverage, we attach the transmitter and receiver to the walls as shown in Fig. 22(d). Now the whole area can be covered for walking detection.

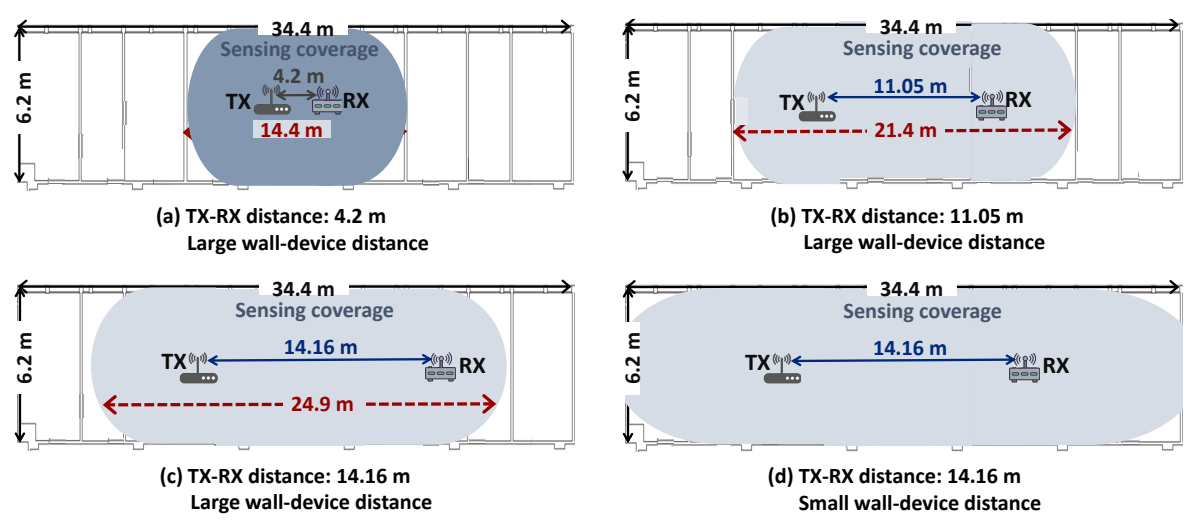


Fig. 22. Enlarging sensing coverage for human walking detection with devices inside rooms.

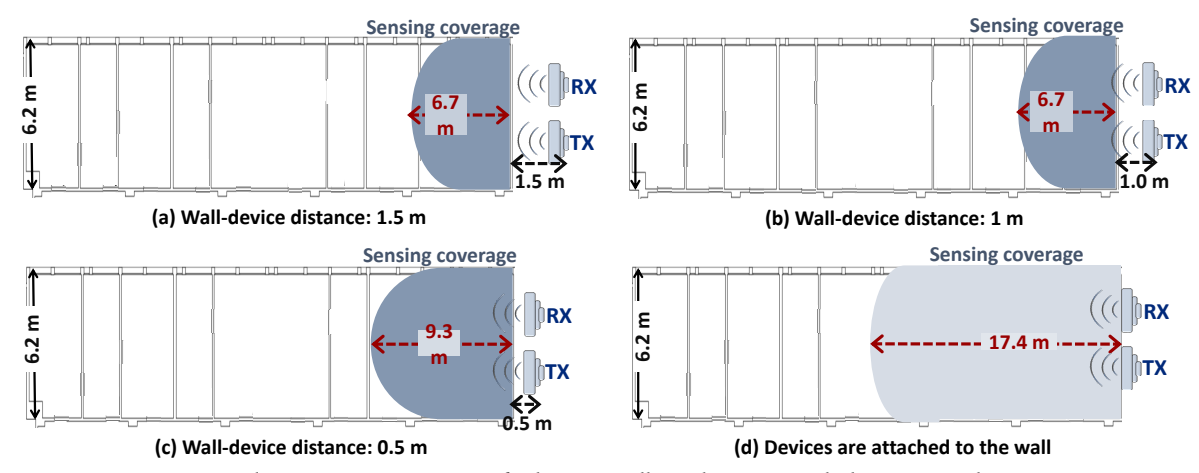


Fig. 23. Enlarging sensing coverage for human walking detection with devices outside rooms.

**Case II: devices are located outside targeted rooms.** In this experiment, we deploy one pair of transmitter and receiver outside the rooms to sense the target movement inside. For instance, the eavesdropper places devices

outside a house to track the occupants' daily activities [23]. In this case, directional antennas are employed to focus sensing only in the area of interest. The gain of directional antennas employed in our experiments is 8 dBi [3]. We compare the sensing coverages under four different deployments as shown in Fig. 23. When the wall-device distance is 1.5 m (Fig. 23(a)), the sensing coverage is only 6.7 m  $\times$  6.2 m. When we reduce the wall-device distance to 1 m (Fig. 23(b)), the size of sensing coverage has little change. In Fig. 23(c), we further decrease the wall-device distance to 0.5 m, and we observe that the size of sensing coverage increases to around 9.3 m  $\times$  6.2 m. As shown in Fig. 23(d), when we attach the devices to the wall, the sensing coverage is increased significantly to around 17.4 m  $\times$  6.2 m. Now the size of sensing coverage is increased by around 160% compared to that with a wall-device distance of 1.5 m. These experiments demonstrate the effectiveness of leveraging wall-device distance to enlarge the sensing coverage for walking detection.

# 5.3 Mitigating Interference

For interference mitigation, we also conduct experiments with two applications, i.e., micro-level respiration monitoring and macro-level walking sensing.

- 5.3.1 Respiration Monitoring in the Presence of Interference. We evaluate the impact of interference on respiration sensing as shown in Fig. 24 where the target is sitting in one room while three interferers are randomly walking outside the room. We conduct experiments under two different deployments.
  - Deployment I: as shown in Fig. 24(a), we place the transmitter and receiver at a small distance of 8 m with only one wall in between. Under this deployment, the sensing coverage is large and can cover both the target and interferers.
  - Deployment II: as shown in Fig. 24(b), we place the transmitter in one room around 20 m away from the receiver with two walls in between. Under this deployment, the sensing coverage becomes smaller highlighted in blue color. The target is now located inside the sensing coverage while three interferers are outside the sensing coverage.

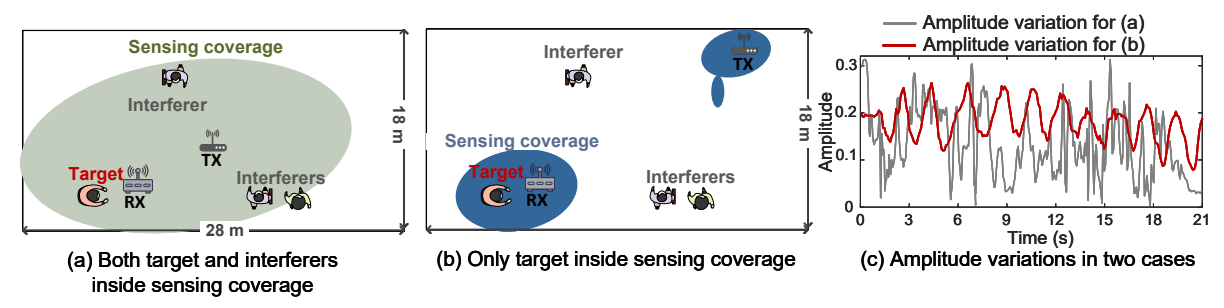


Fig. 24. Respiration sensing in the presence of interference.

To evaluate the performance of mitigating interference, we present the respiration-induced amplitude variations for these two deployments as shown in Fig. 24(c). We can see that when the interferers are also located inside the sensing coverage, i.e., under Deployment I, they severely distort the respiration pattern of the target. The distorted signal is highlighted in grey. On the other hand, when only the target is located inside the sensing coverage, i.e., under Deployment II, we can obtain clear periodic respiration pattern highlighted in red. The interferers' walking does not cause interference to target sensing in this setup. This experiment demonstrates the effectiveness of planning device placement to mitigate interference.

- 5.3.2 Walking Sensing in the Presence of Interference. In this section, we further conduct experiments under two different deployments as presented in Fig. 25. The target is walking in the hallway while four interferers are located nearby. Among these four interferers, three interferers are walking and the other one is sitting.
  - Deployment I: as shown in Fig. 25(a), we place the transmitter in the same hallway 15 m away from the receiver. The sensing coverage is large enough to cover the interferers as well as the target.
  - Deployment II: as shown in Fig. 25(b), we place the transmitter in one room around 30 m away from the receiver with one wall in between. In this deployment, only the target is located inside the sensing coverage.

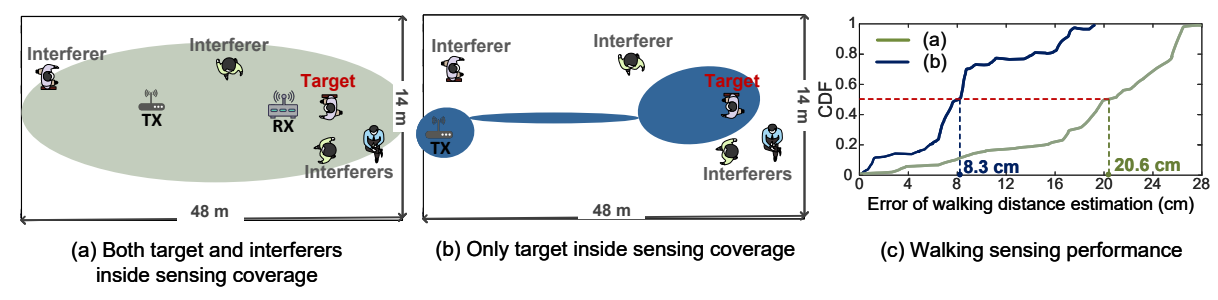


Fig. 25. Walking sensing in the presence of interference.

For each deployment, we conduct 20 experiments and ask the target to walk. The distance between the target and the receiver is in the range of [1 m, 10 m]. We estimate relative walking distance [39] in this application. The ground truth is recorded with a Leica Disto E7300 laser distance meter. The experiment results are shown in Fig. 25(c). We can observe that by making interferers outside the sensing coverage, the error of walking distance estimation is decreased from 20.6 cm to 8.3 cm. This result further validates that interference can be mitigated by controlling the size of sensing coverage.

# 6 DISCUSSION

In this section, we briefly discuss the limitations and future directions of our work.

Wall properties. The size of sensing coverage can be affected by the wall properties including size, material and thickness. This is because these wall properties have a great impact on the signal attenuation induced by the wall. Our proposed through-wall sensing coverage model is general, and we do not evaluate the impact of these properties. Researchers have presented empirical measurements on signal attenuation caused by walls made of different materials (e.g., brick and concrete walls) [19]. Moreover, the works in the field of material sensing [24, 32] also provide insights on the impact of wall properties on signal attenuation. These works can help refine the through-wall sensing model further.

Non-parallel walls. In the multi-wall scenarios, we assume the walls are parallel to each other. In real-world scenarios, the walls may not always be parallel and the floor plan can be more complicated. Based on our simulation, with non-parallel walls, the sensing coverage still increases when the transmitter/receiver is placed close to a wall. The shape is different from that with parallel walls. We hope that our research can inspire follow-up investigation on wireless sensing with non-parallel walls.

Impact of door open and closed on sensing coverage. To evaluate the sensing coverage of through-wall scenarios, we conduct experiments in indoor environments with multiple rooms. We observe that when the doors of these rooms are open, the sensing coverage is larger than that when the doors are closed. We believe that this is because some signals can penetrate the doors and propagate in the hallway before arriving at the receiver. When the doors are open, the signals penetrating the doors experience less attenuation, resulting in a larger sensing coverage.

Other benefits on sensing by leveraging the effect of walls. Making good use of walls can bring a large range of benefits on sensing. We briefly discuss a few benefits here. (1) Whole apartment sensing. For applications such as fall detection, a larger sensing coverage is preferred. If we do not properly place the devices, one pair of transmitter and receiver can only cover a small area inside the apartment. By leveraging the findings to place the devices carefully, the whole apartment can be covered. (2) Precise sensing. By placing the sensing device properly, we can confine sensing within the area of interest. For example, for sleep monitoring, we want sensing to be constrained within the bedroom without being interfered by activities happening in the living room. (3) Sensing with mobility. One direction of wireless sensing is to place the sensing device on mobile platforms such as a robot for sensing [17, 30, 41]. We envision the effect of wall can help the robot identify locations to achieve optimal sensing performance in indoor environment.

#### 7 RELATED WORK

In this section, we discuss the most related work in the following domains.

Wireless sensing through walls and occlusions. In the last few years, various wireless signals have been utilized for through-wall sensing, including Radar [4, 43-46], WiFi [5, 13, 15, 21, 22, 26, 28, 38], RFID [24, 36] and acoustic [18]. These systems are typically designed for applications such as imaging, tracking, capturing body shape, and mesh construction. However, the sensing coverage is limited. Moreover, they do not explore how the wall changes the signal reflections and affects sensing. In contrast, we develop a through-wall sensing model to characterize the effect of wall on wireless sensing. Zhang et al. investigate the impact of wall on the Fresnel zone model [42]. Different from this work, we explore a new direction and study how to leverage the wall to enlarge the sensing coverage and mitigate interference.

Modeling sensing coverage without walls. The sensing coverage model without walls has been well studied in Radar and WiFi systems. Wang et al. [25] model the coverage of WiFi sensing when the transmitter and receiver are deployed in the same room. Woodford et al. [27] leverage the reflector geometries to extend the sensing coverage of Radar around the corner to avoid traffic collisions. Yang et al. [37] study how the sensing coverage of Radar systems changes with respect to the distance between transmitter and receiver. However, they mainly consider scenarios where there is no wall between the target and device. This is mainly because the through-wall capability of WiFi sensing and Radar sensing is limited. Different from these works, we model the through-wall sensing coverage of LoRa and provide insight on how to leverage the wall to control the sensing coverage.

Sensing coverage of LoRa. LoRa has been employed for wireless sensing owning to the long transmission distance and through-wall sensing capability of LoRa signals. Chen et al. [8] place LoRa devices on a drone to detect the presence of human targets inside a building. Zhang et al. [39] employ the signal ratio scheme to increase the sensing range to around 25 m. They also adopt the beamforming technique with four antennas at the LoRa receiver to achieve multi-target respiration sensing [40]. Xie et al. further improve the sensing range and also mitigate the interference issue [29, 31, 34]. However, these works do not quantify the sensing coverage in through-wall scenarios. Chang et al. utilize the long transmission range of LoRa for soil sensing [7], which is not contact-free sensing that our proposed method is designed for.

# CONCLUSION

In this work, we rethink the effect of wall on through-wall sensing and discover the fact that walls do not always decrease but sometimes can increase the sensing coverage. We show that the through-wall sensing coverage is closely related to three factors, i.e., the wall-device distance, transmitter-receiver distance, and the number of walls. Based on these factors, we provide insights on how to plan the device placement to enlarge sensing coverage and mitigate interference. We believe the proposed theories can help guide the real-world deployment of through-wall sensing systems. Such a through-wall sensing coverage model can be extended to benefit the design of other wireless sensing systems such as WiFi, UWB and mmWave.

#### **ACKNOWLEDGMENTS**

This work was partially supported by the NSF under Grant CAREER-2144668 and UMass Amherst Institute For Applied Life Sciences (IALS) Equipment Fund. Binbin Xie is supported by Google PhD Fellowship in Mobile Computing.

#### REFERENCES

- [1] Friis transmission equation. https://www.antenna-theory.com/basics/friis.php.
- [2] Proxicast antenna. https://www.proxicast.com/support/files/ant-120-006-specifications.pdf.
- [3] Rfmax directional antenna. https://rfid.atlasrfidstore.com/hs-fs/hub/300870/file-1486000779-pdf/tech\_spec\_sheets/laird/atlas\_laird\_s8658 p\_antenna-1.pdf.
- [4] F. Adib, C.-Y. Hsu, H. Mao, D. Katabi, and F. Durand. Capturing the human figure through a wall. ACM Transactions on Graphics (TOG), 34(6):1–13, 2015.
- [5] F. Adib and D. Katabi. See through walls with wifi! In ACM Special Interest Group on Data Communication (SIGCOMM), pages 75–86. ACM, 2013.
- [6] T. I. O. Ahmed and M. Mirghani. Estimation of radar cross sectional area of target using simulation algorithm. *International Journal of Research Studies in Electrical and Electronics Engineering*, 4(2), 2018.
- [7] Z. Chang, F. Zhang, J. Xiong, J. Ma, B. Jin, and D. Zhang. Sensor-free soil moisture sensing using lora signals. ACM on Interactive, Mobile, Wearable and Ubiquitous Technologies (IMWUT), 6(2):1–27, 2022.
- [8] L. Chen, J. Xiong, X. Chen, S. I. Lee, K. Chen, D. Han, D. Fang, Z. Tang, and Z. Wang. Widesee: towards wide-area contactless wireless sensing. In 17th Conference on Embedded Networked Sensor Systems (SenSys), pages 258–270. ACM, 2019.
- [9] X. Chen, D. Ganesan, J. Gummeson, and M. Rostami. Cocoon: A conductive substrate-based coupled oscillator network for wireless communication. In 19th ACM Conference on Embedded Networked Sensor Systems (SenSys), pages 84–96. ACM, 2021.
- [10] M. Cui, B. Xie, Q. Wang, and J. Xiong. Dancingant: Body-empowered wireless sensing utilizing pervasive radiations from powerline. In 29th Annual International Conference on Mobile Computing And Networking (MobiCom), pages 873–887. ACM, 2023.
- [11] M. Dunna, C. Zhang, D. Sievenpiper, and D. Bharadia. Scattermimo: Enabling virtual mimo with smart surfaces. In 26th Annual International Conference on Mobile Computing and Networking (MobiCom), pages 1–14. ACM, 2020.
- [12] N. Hosseini, M. Khatun, C. Guo, K. Du, O. Ozdemir, D. W. Matolak, I. Guvenc, and H. Mehrpouyan. Attenuation of several common building materials: millimeter-wave frequency bands 28, 73, and 91 ghz. *IEEE Antennas and Propagation Magazine*, 63(6):40–50, 2021.
- [13] W. Jiang, H. Xue, C. Miao, S. Wang, S. Lin, C. Tian, S. Murali, H. Hu, Z. Sun, and L. Su. Towards 3d human pose construction using wifi. In 26th Annual International Conference on Mobile Computing and Networking (MobiCom), pages 1–14. ACM, 2020.
- [14] A. Kamann, P. Held, F. Perras, P. Zaumseil, T. Brandmeier, and U. T. Schwarz. Automotive radar multipath propagation in uncertain environments. In 21st International Conference on Intelligent Transportation Systems (ITSC), pages 859–864. IEEE, 2018.
- [15] C. R. Karanam and Y. Mostofi. 3d through-wall imaging with unmanned aerial vehicles using wifi. In 16th ACM/IEEE International Conference on Information Processing in Sensor Networks (IPSN), pages 131–142. IEEE, 2017.
- [16] J. C. Liando, A. Gamage, A. W. Tengourtius, and M. Li. Known and unknown facts of lora: Experiences from a large-scale measurement study. ACM Transactions on Sensor Networks, 15(2):1–35, 2019.
- [17] J. Liu, D. Li, L. Wang, F. Zhang, and J. Xiong. Enabling contact-free acoustic sensing under device motion. ACM on Interactive, Mobile, Wearable and Ubiquitous Technologies (IMWUT), 6(3):1–27, 2022.
- [18] W. Mao, M. Wang, and L. Qiu. Aim: Acoustic imaging on a mobile. In 16th International Conference on Mobile Systems, Applications, and Services (MobiSys), pages 468–481. ACM, 2018.
- [19] D. Pena, R. Feick, H. D. Hristov, and W. Grote. Measurement and modeling of propagation losses in brick and concrete walls for the 900-mhz band. *IEEE Transactions on Antennas and Propagation*, 51(1):31–39, 2003.
- [20] Z. Peng, L. Li, M. Wang, Z. Zhang, Q. Liu, Y. Liu, and R. Liu. An effective coverage scheme with passive-reflectors for urban millimeter-wave communication. IEEE Antennas and Wireless Propagation Letters, 15:398–401, 2015.
- [21] Y. Ren, Z. Wang, S. Tan, Y. Chen, and J. Yang. Winect: 3d human pose tracking for free-form activity using commodity wifi. ACM on Interactive, Mobile, Wearable and Ubiquitous Technologies (IMWUT), 5(4):1–29, 2021.
- [22] Y. Ren, Z. Wang, Y. Wang, S. Tan, Y. Chen, and J. Yang. Gopose: 3d human pose estimation using wifi. ACM on Interactive, Mobile, Wearable and Ubiquitous Technologies (IMWUT), 6(2):1–25, 2022.
- [23] J. Shenoy, Z. Liu, B. Tao, Z. Kabelac, and D. Vasisht. Rf-protect: privacy against device-free human tracking. In ACM Special Interest Group on Data Communication (SIGCOMM), pages 588–600. ACM, 2022.

- [24] J. Wang, J. Xiong, X. Chen, H. Jiang, R. K. Balan, and D. Fang. Tagscan: Simultaneous target imaging and material identification with commodity rfid devices. In The 23rd Annual International Conference on Mobile Computing and Networking, pages 288-300. ACM, 2017.
- [25] X. Wang, K. Niu, J. Xiong, B. Qian, Z. Yao, T. Lou, and D. Zhang. Placement matters: Understanding the effects of device placement for wifi sensing. ACM on Interactive, Mobile, Wearable and Ubiquitous Technologies (IMWUT), 6(1):1-25, 2022.
- [26] Y. Wang, Y. Ren, Y. Chen, and J. Yang. A wifi vision-based 3d human mesh reconstruction. In 28th Annual International Conference on Mobile Computing and Networking (MobiCom), pages 814–816, 2022.
- [27] T. Woodford, X. Zhang, E. Chai, and K. Sundaresan. Mosaic: leveraging diverse reflector geometries for omnidirectional around-corner automotive radar. In The 20th Annual International Conference on Mobile Systems, Applications and Services (MobiSys), pages 155-167. ACM, 2022.
- [28] C. Wu, F. Zhang, Y. Hu, and K. R. Liu. Gaitway: Monitoring and recognizing gait speed through the walls. IEEE Transactions on Mobile Computing (TMC), 20(6):2186-2199, 2020.
- [29] B. Xie, M. Cui, D. Ganesan, X. Chen, and J. Xiong. Boosting the long range sensing potential of lora. In Proceedings of the 21st Annual International Conference on Mobile Systems, Applications and Services (MobiSys), pages 177-190. ACM, 2023.
- [30] B. Xie, D. Ganesan, and J. Xiong. Embracing lora sensing with device mobility. In 20th ACM Conference on Embedded Networked Sensor Systems (SenSys), pages 349-361. ACM, 2022.
- [31] B. Xie and J. Xiong. Combating interference for long range lora sensing. In 18th ACM Conference on Embedded Networked Sensor Systems (SenSys), pages 69-81. ACM, 2020.
- [32] B. Xie, J. Xiong, X. Chen, E. Chai, L. Li, Z. Tang, and D. Fang. Tagtag: material sensing with commodity rfid. In 17th Conference on Embedded Networked Sensor Systems (SenSys), pages 338–350. ACM, 2019.
- [33] B. Xie, J. Xiong, X. Chen, and D. Fang. Exploring commodity rfid for contactless sub-millimeter vibration sensing. In 18th Annual International Conference on Embedded Networked Sensor Systems (SenSys), pages 15-27. ACM, 2020.
- [34] B. Xie, Y. Yin, and J. Xiong. Pushing the limits of long range wireless sensing with lora. ACM on Interactive, Mobile, Wearable and Ubiquitous Technologies (IMWUT), 5(3):1-21, 2021.
- [35] H. Xue, Y. Ju, C. Miao, Y. Wang, S. Wang, A. Zhang, and L. Su. mmmesh: Towards 3d real-time dynamic human mesh construction using millimeter-wave. In 19th International Conference on Mobile Systems, Applications, and Services (MobiSys), pages 269-282. ACM, 2021.
- [36] L. Yang, Q. Lin, X. Li, T. Liu, and Y. Liu. See through walls with cots rfid system! In 21st Annual International Conference on Mobile Computing And Networking (MobiCom), pages 487–499. ACM, 2015.
- [37] Q. Yang, S. He, and J. Chen. Energy-efficient area coverage in bistatic radar sensor networks. In IEEE Global Communications Conference (GLOBECOM), pages 280-285. IEEE, 2013.
- [38] D. Zhang, J. Wang, J. Jang, J. Zhang, and S. Kumar. On the feasibility of wi-fi based material sensing. In 25th Annual International Conference on Mobile Computing and Networking (MobiCom), pages 1-16. ACM, 2019.
- [39] F. Zhang, Z. Chang, K. Niu, J. Xiong, B. Jin, Q. Lv, and D. Zhang. Exploring lora for long-range through-wall sensing. ACM on Interactive, Mobile, Wearable and Ubiquitous Technologies (IMWUT), 4(2):1-27, 2020.
- [40] F. Zhang, Z. Chang, J. Xiong, R. Zheng, J. Ma, K. Niu, B. Jin, and D. Zhang. Unlocking the beamforming potential of lora for long-range multi-target respiration sensing. ACM on Interactive, Mobile, Wearable and Ubiquitous Technologies (IMWUT), 5(2):1-25, 2021.
- [41] F. Zhang, J. Xiong, Z. Chang, J. Ma, and D. Zhang. Mobi2sense: empowering wireless sensing with mobility. In 28th Annual International Conference on Mobile Computing And Networking (MobiCom), pages 268-281. ACM, 2022.
- [42] H. Zhang, Z. Wang, Z. Sun, W. Song, Z. Ren, Z. Yu, and B. Guo. Understanding the mechanism of through-wall wireless sensing: A model-based perspective. ACM on Interactive, Mobile, Wearable and Ubiquitous Technologies (IMWUT), 6(4):1-28, 2023.
- [43] M. Zhao, T. Li, M. Abu Alsheikh, Y. Tian, H. Zhao, A. Torralba, and D. Katabi. Through-wall human pose estimation using radio signals. In IEEE/CVF International Conference on Computer Vision (CVPR), pages 7356-7365. IEEE/CVF, 2018.
- [44] M. Zhao, Y. Liu, A. Raghu, T. Li, H. Zhao, A. Torralba, and D. Katabi. Through-wall human mesh recovery using radio signals. In IEEE/CVF International Conference on Computer Vision (CVPR), pages 10113-10122. IEEE/CVF, 2019.
- [45] M. Zhao, Y. Tian, H. Zhao, M. A. Alsheikh, T. Li, R. Hristov, Z. Kabelac, D. Katabi, and A. Torralba. Rf-based 3d skeletons. In ACM Special Interest Group on Data Communication (SIGCOMM), pages 267–281. ACM, 2018.
- [46] T. Zheng, Z. Chen, J. Luo, L. Ke, C. Zhao, and Y. Yang. Siwa: see into walls via deep uwb radar. In Annual International Conference on Mobile Computing and Networking (MobiCom), pages 323–336. ACM, 2021.

#### A APPENDIX

Here we explain why the proposed sensing model in Section 3.1 characterizes the received signal power using the product of distances instead of the sum of distances.

Note that our model characterizes the received signal power  $P_r$  in Fig. 26 using the product distances  $d_1d_2$ , which can be simplified as

$$P_r \propto \frac{1}{d_1 d_2}$$

where  $d_1$  is the transmitter-wall distance and  $d_2$  is the wall-receiver distance. On the other hand, another model [19] uses the sum of distances to characterize the received signal power  $P_r$ , which can be represented as

$$P_r \propto \frac{1}{d_1 + d_2}.$$

Both of these two models are correct, but have different assumptions. Specifically, the second model assumes the beam diameter at the wall is smaller than the size of wall [12, 19] as shown in Fig. 27(a). To make this assumption valid, the distance between the transmitter and receiver is kept very small (e.g., 1.3 m) [19]. As shown in Fig. 27(a), when the distance between transmitter and receiver is small, the beam size at the wall is smaller than the wall. In the context of long range sensing which our system is designed for, the distance between transmitter and receiver is much larger (e.g., 10 m and 18 m). As shown in Fig. 27(b), when the distance between transmitter and receiver is large, the beam size at the wall is not smaller than the wall size. In this case, the assumption in the second model [19] does not hold. For this scenario, we employ the product of distances (i.e., transmitter-wall distance and wall-receiver distance) to quantify the received signal power.

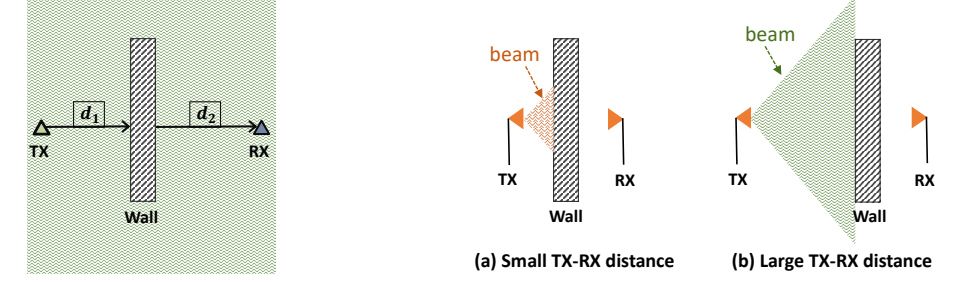


Fig. 26. A simple scenario for Fig. 27. The beam diameter varies with the transmitter-receiver distance. analyzing the effect of wall.